AWARD NUMBER: W81XWH-15-1-0056

TITLE: Do Prostate Cancer Exosomes Generate a Field Effect leading to Tumor Multifocality?

PRINCIPAL INVESTIGATOR: Marco Bisoffi, PhD

CONTRACTING ORGANIZATION: Chapman University, Orange, CA 92866

REPORT DATE: April 2016

TYPE OF REPORT: Annual

PREPARED FOR: U.S. Army Medical Research and Materiel Command
Fort Detrick, Maryland 21702-5012

REPORT DOCUMENTATION PAGE

Form Approved
OMB No. 0704-0188

1. REPORT DATE	**2. REPORT TYPE**	**3. DATES COVERED**
April 2016	Annual	03/25/2015 – 03/24/2016

4. TITLE AND SUBTITLE

Do Prostate Cancer Exosomes Generate a Field Effect leading to Tumor Multifocality?

5a. CONTRACT NUMBER

5b. GRANT NUMBER
W81XWH-15-1-0056

5c. PROGRAM ELEMENT NUMBER

6. AUTHOR(S)

Marco Bisoffi

E-Mail: bisoffi@chapman.edu

5d. PROJECT NUMBER

5e. TASK NUMBER

5f. WORK UNIT NUMBER

7. PERFORMING ORGANIZATION NAME(S) AND ADDRESS(ES)

Chapman University, Schmid College of Science and Technology
Biochemistry and Molecular Biology Division
1 University Drive
92866 Orange CA

8. PERFORMING ORGANIZATION REPORT NUMBER

9. SPONSORING / MONITORING AGENCY NAME(S) AND ADDRESS(ES)

U.S. Army Medical Research and Materiel Command
Fort Detrick, Maryland 21702-5012

10. SPONSOR/MONITOR'S ACRONYM(S)

11. SPONSOR/MONITOR'S REPORT NUMBER(S)

12. DISTRIBUTION / AVAILABILITY STATEMENT

Approved for Public Release; Distribution Unlimited

13. SUPPLEMENTARY NOTES

14. ABSTRACT

Prostate field effect (or field cancerization) denotes the presence of molecular aberrations featured in structurally intact cells of histologically normal tissues adjacent to adenocarcinomas, in many cases as distant as centimeters from the tumor margin. The presence of a field effect is causatively associated with the occurrence of tumor multifocality in the prostate, but a notable gap of knowledge is the lack of understanding of how multifocal fields of molecular aberrations in histologically normal tissues adjacent to tumors form. We propose a novel line of investigation that will implicate exosomes, extracellular vesicles secreted by prostate epithelial cells, in the formation of field effect and tumor multifocality. The Specific Aims are (i) to test the effect of prostate cancer exosomes on non-cancerous cells and (ii) to determine the association between markers of field effect and markers of exosomes in tissues adjacent to adenocarcinomas. Accomplishments so far include (i) the isolation and partial characterization of exosomes from prostate cells, (ii) the determination of the effect of prostate cancer cell exosomes on markers of field effect in normal cells, (iii) the completion of a manuscript, and (iv) building strategically meaningful alliances.

15. SUBJECT TERMS
Prostate cancer exosomes, field effect, tumor multifocality, preliminary data, strategic alliances, manuscript.

16. SECURITY CLASSIFICATION OF:			**17. LIMITATION OF ABSTRACT**	**18. NUMBER OF PAGES**	**19a. NAME OF RESPONSIBLE PERSON**
a. REPORT	**b. ABSTRACT**	**c. THIS PAGE**			USAMRMC
U	U	U	UU	38	**19b. TELEPHONE NUMBER** *(include area code)*

Table of Contents

1. Introduction

Prostate field effect (or field cancerization) denotes the presence of molecular aberrations featured in structurally intact cells of histologically normal tissues adjacent to adenocarcinomas, in many cases as distant as centimeters from the tumor margin. Prostate field effect is increasingly accepted as a type of molecular pathology with potentially far-reaching clinical implications (see Impact below). The presence of a field effect is causatively associated with the occurrence of tumor multifocality in the prostate, but a notable gap of knowledge is the lack of understanding of how multifocal fields of molecular aberrations in histologically normal tissues adjacent to tumors form. We propose a novel line of investigation by combining for the first time the concept of field effect with the concept of exosome trafficking. Exosomes are a type of extracellular nanovesicles that are secreted by prostate epithelial cells, and that carry a multitude of factors that affect cellular physiology. In grant W81XWH-15-1-0056e we hypothesize a novel, as yet unexplored role of prostate cancer exosomes, namely that they are "messengers" of field formation in histologically normal tissues adjacent to adenocarcinomas, and that their "cargo" primes areas outside of the tumor margin for additional tumor development (figure). This venue has not been previously pursued and represents an entirely new line of questioning. The rationale for this is based on the premise that exosomes carry factors that can alter the physiology of cells and tissues at greater distances. By extension, they could induce markers and mediators of tumorigenesis in histologically normal tissues adjacent to solid tumors, or a field effect. In agreement with the scope of an Exploration - Hypothesis Development Award, the objective is to test our hypothesis for the generation of preliminary data that will justify more translational follow-up studies with preclinical character.

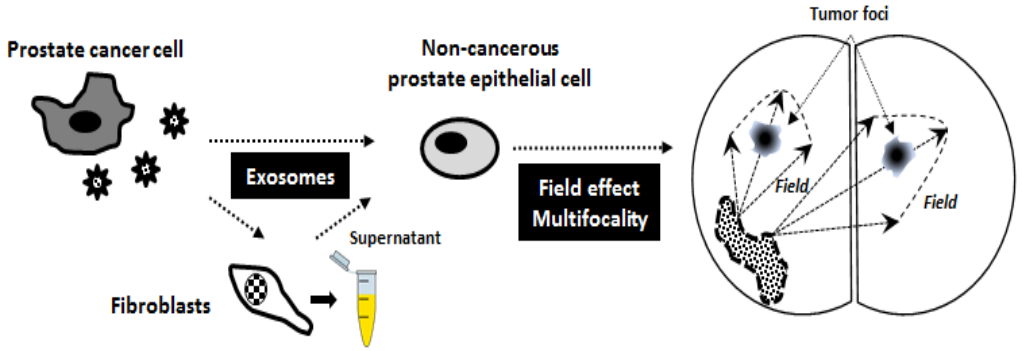

Specific Aim 1: To test the effect of prostate cancer exosomes on non-cancerous cells. The specific tasks of Aim 1 are to determine whether prostate cancer exosomes induce markers characteristic of field effect and whether such activation induces elevated proliferation and/or reduced apoptosis.

Specific Aim 2: To determine the association between markers of field effect and markers of exosomes in tissues adjacent to adenocarcinomas. The specific tasks of Aim 2 are to determine whether the presence and expression level of markers of field effect and markers of exosomes correlate in tumor adjacent tissues; and to assess whether these parameters differ in adjacent tissues derived from unifocal *vs.* multifocal prostate cancers.

2. Keywords

Prostate cancer, tumor multifocality, field effect, exosomes.

3. Accomplishments

Essential experimental data pertinent to the goals of Specific Aim 1, as well as strategic alliances were achieved during the first period covered by grant W81XWH-15-1-0056. The following are representative examples:

(i) Isolation and partial characterization of exosomes from prostate cells.

We have adopted an ultracentrifugation based protocol for the isolation of exosomes from a variety of human prostate cell models, including the non-cancerous RWPE-1 and the cancerous LNCaP and PC-3 cells. The figure below shows the protein profiles, as revealed by sodium dodecyl sulfate polyacrylamide gel electrophoresis (SDS-PAGE) (left) and visualization by light scattering of exosomes isolated from LNCaP and

PC-3 cells (right). Further biochemical characterization to confirm the identity and content of theses vesicles are under way.

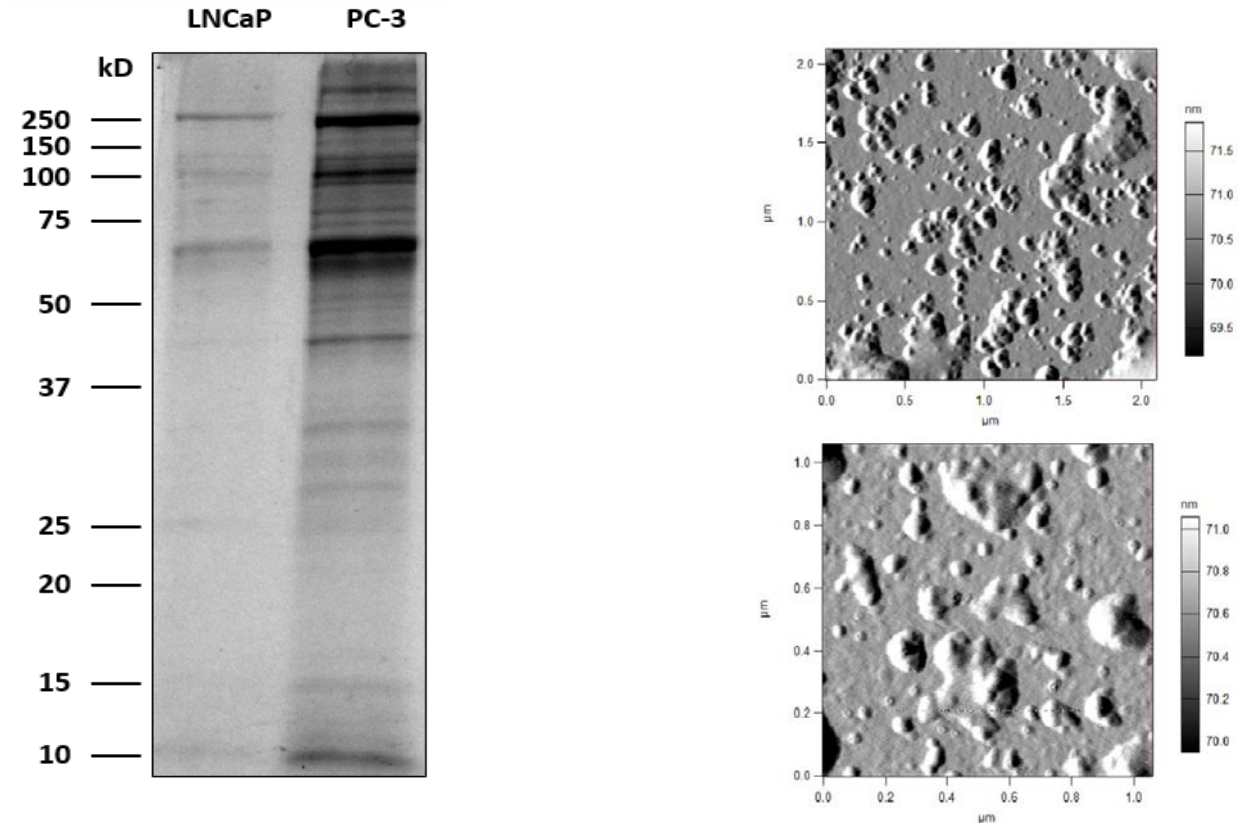

(ii) Effect of prostate cancer cell exosomes on markers of filed effect in normal cells.

We have started to explore the effect of exosomes released from prostate cancer cells (LNCaP and PC-3) on the cells of the non-cancerous phenotype (RWPE-1). In particular, we are interested in determining whether such exosomes can induce established markers of field effect, including the ones that we have reported previously, such as early growth response 1 (EGR-1), macrophage inhibitory cytokine 1 (MIC-1), platelet derived growth factor A (PDGF-A), and fatty acid synthase (FASN). The figure below shows the effect of LNCaP and PC-3 released exosomes on the mRNA expression of EGR-1, MIC-1, PDGF-A, and FASN in RWPE-1. While there is variation, this data indicates that exosomes released from prostate cancer cells induce markers of file effect in normal cells. Current experiments include testing phenotypic effects, such as proliferation/cell death and cell motility.

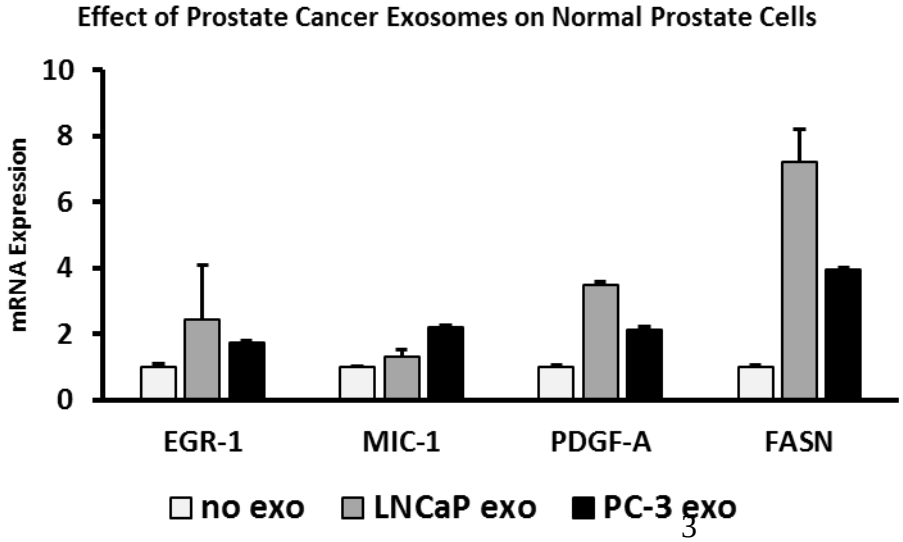

(iii) Completion of a manuscript (submitted).

We decided to strengthen the rationale for the choice of markers of prostate field effect with respect to the experimental approaches in Specific Aim 2, where we will utilize valuable human tissues, including tissue samples purchased from commercial sources (such as the Cooperative Human Tissue Network), as well as tissue samples from the PI's own repository. Accordingly, our efforts during the first time period covered by grant W81XWH-15-1-0056 included the completion of an extensive association analysis between the four prominent protein markers of prostate field effect, i.e. EGR-1, MIC-1, PDGF-A, and FASN. This is important for example because EGR-1 and PDGF-A are featured centrally in the Specific Aims of W81XWH-15-1-0056. This effort not only revalidated the choice of these markers, but in addition led to the submission of a manuscript entitled *"Association and regulation of protein factors of field effect in prostate tissues"* by Kristin N. Gabriel, Anna C. Jones, Kresta S. Antillon, Sara N. Janos, Heidi N. Overton, Shannon M. Jenkins, Emily H. Frisch, Julie PT Nguyen, Kristina A. Trujillo, and Marco Bisoffi. The manuscript has been favorably reviewed by the *International Journal of Oncology* (manuscript ID 167557-IJO) and is currently under revision nearing re-submission. The revised manuscript is provided in the Appendices of this report. Importantly, grant support from W81XWH-15-1-0056 is acknowledged in this publication. We feel that the completion of this manuscript was important for ensuring the success of the remaining upcoming investigations.

(iv) Building strategically meaningful alliances.

To strengthen the goals and ensure the successful completion of proposal W81XWH-15-1-0056, we have established professional connections. Accordingly, we reached out to leaders in the field of prostate molecular pathology and clinical science. In particular, successful connections with the following individuals and teams were made:

- Dan Mercola, MD/PhD, Department of Pathology, University of California at Irvine (UCI), CA. Dr. Mercola is an internationally known leader in prostate biomarkers, and directs a National Institutes of Health supported tissue repository. Dr. Mercola has invited the PI to present at UCI and has offered access to tissue samples to support his research.

- Veronique Baron, PhD, Vaccine Research Institute of San Diego, CA. Dr. Baron is an expert in EGR-1 biology and has taken an interest in the PI's efforts to elucidate the etiology and role of this transcription factor in prostate field effect.

- Genitourinary disease oriented team (GU-DOT) at the UCI Chao Family Comprehensive Cancer Center (UCICCC) in Orange CA. The GU-DOT is led by a consortium of clinicians and translational researchers. The PI (Marco Bisoffi) has become an Associate Member of the UCICCC and has presented and discussed his research at GU-DOT and at the UCICCC Annual Retreat.

The PI feels that it was important to add expertise, support, and resources to optimize the continuation and completion of the work planned in grant proposal W81XWH-15-1-0056.

4. Impact

The impact of the present research is represented by its responsiveness to the PCRP Overarching Challenges *"Develop better tools for early detection of clinically relevant disease"*, *"Distinguish aggressive from indolent disease in men newly diagnosed with prostate cancer"*, and *"Tumor and Microenvironment Biology: Understanding prognosis and progression of prostate cancer"*. Multifocality is a major contributor to the complexity and inaccuracy of all aspects of prostate cancer clinical assessment and management. It complicates staging and grading because of increased heterogeneity, and can bar focal therapy for patients with low risk disease (defined as Gleason grade $\leq$6 and a PSA of <10 ng/ml), which represent 40-50% of newly diagnosed prostate cancer cases in populations where screening is part of the standard of care. Focal therapy is an organ-

sparing therapeutic intervention by different means aimed at avoiding the side effects of radical therapies which can lower the quality of life. It is complementary to active surveillance and is becoming increasingly accepted as part of the effort of developing personalized approaches for prostate cancer patients in the 21st century. Towards this goal, a detailed understanding of the etiology of tumor multifocality is mandatory. It is conceivable that future therapeutic attempts may include early intervention aimed at inhibiting exosome shedding and distant tumor formation to suppress multifocality. Proven markers and mediators of field effect could also be used for the detection of tissue areas prone to the formation of tumor foci.
In summary, data emerging from this work will justify studies in mouse models of prostate cancer with more mechanistic character. Should our work indicate a strong association between markers of field effect and the presence of exosomes, we will design in vivo experiments with orthotopically implanted prostate cancer cells genetically modified to induce a field effect and test for the formation of multifocality. We foresee that such mechanistic / functional work could lead to the development of new and early markers of disease and modes of intervention.

5. Changes / Modifications
A notable change is that the PI has requested a no-cost extension for grant proposal W81XWH-15-1-0056. As of July 27, 2016, this request has been granted and the final report date has been set for June 2017. Most of the remaining work supported by grant proposal W81XWH-15-1-0056 pertains to investigations outlined under Specific Aim 2. The major goal is to determine the association between markers of field effect and markers of exosomes in tissues adjacent to adenocarcinomas. The specific tasks of Aim 2 are:

- To determine whether the presence and expression level of markers of field effect and markers of exosomes correlate in tumor adjacent tissues.
- To assess whether these parameters differ in adjacent tissues derived from unifocal *vs.* multifocal prostate cancers.

The PI's experimental observations so far and the added expertise, support, and resources from the PI's newly established connections should be essential in helping complete the remaining planned work.

6. Products
None to report.

7. Participants & Other Collaborating Organizations
The work proposed in grant proposal W81XWH-15-1-0056 continues to be performed at Chapman University, Schmid College of Science and Technology, Biochemistry and Molecular Biology Division, where the PI (Marco Bisoffi) has established a new research program.
In addition, in preparation of the work outlined in Specific Aim 2, the PI has established a professional connection with Dan Mercola, MD/PhD, Department of Pathology, University of California at Irvine (UCI), CA. Dr. Mercola is an internationally known leader in prostate biomarkers, and directs a National Institutes of Health supported tissue repository. Dr. Mercola has invited the PI to present at UCI and has offered access to tissue samples to support his research.

8. Special Reporting Requirements
None.

9. Appendices

The appendix features a revised manuscript submitted to the International Journal of Oncology (manuscript ID 167557-IJO). The study represents an extensive association analysis between the four prominent protein markers of prostate field effect, i.e. EGR-1, MIC-1, PDGF-A, and FASN and acknowledges support from the W81XWH-15-1-0056 award:

"Association and regulation of protein factors of field effect in prostate tissues" by Kristin N. Gabriel, Anna C. Jones, Kresta S. Antillon, Sara N. Janos, Heidi N. Overton, Shannon M. Jenkins, Emily H. Frisch, Julie PT Nguyen, Kristina A. Trujillo, and Marco Bisoffi.

Blank Page

Association and regulation of protein factors of field effect in prostate tissues

Kristin N. Gabriel,[1,†] Anna C. Jones,[2,†] Julie PT Nguyen,[1] Kresta S. Antillon,[2] Sara N. Janos,[2] Heidi N. Overton,[2] Shannon M. Jenkins,[2] Emily H. Frisch,[1] Kristina A. Trujillo,[3] and Marco Bisoffi[1,2,*]

[1]Chapman University, Schmid College of Science and Technology, Biochemistry and Molecular Biology/ Biological Sciences, Orange, CA
[2]University of New Mexico Health Sciences Center, Department of Biochemistry and Molecular Biology, Albuquerque, NM.
[3]University of New Mexico Health Sciences Center, Department of Cell Biology and Physiology, Albuquerque, NM.

[†] These authors contributed equally to the present work.

Keywords: Prostate cancer, field effect, protein factors

Abbreviations: EGR-1, early growth response 1 (EGR-1); FASN, fatty acid synthase; MIC-1, macrophage inhibitory cytokine 1; PDGF-A, platelet derived growth factor A.

*Correspondence: Marco Bisoffi, Chapman University, Schmid College of Science and Technology, Biochemistry and Molecular Biology, 1 University Drive, Orange, CA 92866. Tel. (417) 516-5961. Email: bisoffi@chapman.edu

Funding Information: This work was supported by National Institutes of Health (NIH) Grant RR0164880, NIH Grant R03CA136030-02, and Department of Defense Prostate Cancer Research Program grant W81XWH-15-1-0056 (to M. Bisoffi), University of New Mexico Cancer Center Support Grant NIH/NCI P30CA118110, grants from the Chapman University Office of Undergraduate Research program (to K. Gabriel and E. Frisch), and a generous gift from Melinda and Edward Subia of Orange County CA.

Abstract

Field effect or field cancerization denotes the presence of molecular aberrations in structurally intact cells residing in histologically normal tissues adjacent to solid tumors. Currently, the etiology of prostate field effect formation is unknown and there is a prominent lack of knowledge of the underlying cellular and molecular pathways. We have previously identified an up-regulated expression of several protein factors representative of prostate field effect, i.e. early growth response 1 (EGR-1), platelet derived growth factor A (PDGF-A), macrophage inhibitory cytokine 1 (MIC-1), and fatty acid synthase (FASN) in tissues at a distance of 1 centimeter from the visible margin of intra-capsule prostate adenocarcinomas. We have hypothesized that the transcription factor EGR-1 could be a key regulator of prostate field effect formation by controlling the expression of PDGF-A, MIC-1, and FASN. Taking advantage of our extensive quantitative immunofluorescence data specific for EGR-1, PDGF-A, MIC-1, and FASN generated in disease-free, tumor adjacent, and cancerous human prostate tissues, we chose comprehensive correlation as our major approach to test this hypothesis. Despite the static nature and sample heterogeneity of association studies, we show here that sophisticated data generation, such as by spectral image acquisition, linear unmixing, and digital quantitative imaging, can provide meaningful indications of molecular regulations in a physiologically relevant *in situ* environment. Our data suggests that EGR-1 acts as a key regulator of prostate field effect through induction of pro-proliferative (PDGF-A and FASN), and suppression of pro-apoptotic (MIC-1) factors. These findings were corroborated by computational promoter analyses and cell transfection experiments in non-cancerous prostate epithelial cells with ectopically induced and suppressed EGR-1 expression. Among several clinical applications, a detailed knowledge of pathways of field effect may lead to the development of targeted intervention strategies preventing progression from pre-malignancy to cancer.

Introduction

Several pre-malignant states of prostate tissues have been previously described to indicate the progression to prostate adenocarcinoma (prostate cancer). Perhaps the most prominent histological deviation from normalcy is prostatic intraepithelial neoplasia (PIN), which can manifest itself as a low or high grade form (1). All forms of PIN are characterized by the presence of intra-luminal proliferation of the secretory cells of the duct acinar system and abnormal cytological features, including the ratio of nuclear-to-cytoplasmic area, size of nucleoli, and chromatin content (2). Another form of pre-malignancy is accepted to be proliferative inflammatory atrophy (PIA), which constitutes a possible link between inflammation and the malignant transformation of prostatic tissues (3). PIA is mainly recognized in low magnification microscopy by a distinct hyperchromatic appearance of glandular components and variable acinar calibers, and a marked presence of inflammatory cells (4). Of note, both PIN and PIA are histologically evident lesions that are identifiable by trained surgical pathologists. However, it is reasonable to postulate that cell morphological changes leading to histologically abnormal appearances of prostate glands are preceded by molecular alterations that occur in complete absence of any cytological or histological change. This definition is in complete agreement with the concept of “field effect” or “field cancerization”, two terms that are used inter-changeably in this report to reflect contemporary research efforts. Originally introduced for renegade cancer cells outside the margins of squamous oral cell carcinoma (5), the updated definition excludes cellular and histological changes and focuses on molecular aberrations (6). Thus, “field cancerized” prostate tissues have been recently characterized by us and others (7-10) by genetic, epigenetic, and biochemical alterations in structurally intact epithelial and stromal cells of histologically normal tissues adjacent to prostate adenocarcinomas.

Along this line, we have recently described four protein factors of prostate field effect. These include the key transcription factor early growth response 1 (EGR-1), the lipogenic enzyme fatty acid synthase (FASN), and the secreted growth factors platelet derived growth factor A (PDGF-A) and macrophage inhibitory cytokine 1 (MIC-1) (11-13). Our previous reports focused on emphasizing the similarity of expression of these factors between tumor tissues and their adjacent tissue areas, thereby supporting the concept of a field effect. Field effect in the prostate has been recognized to be of potential clinical value (7-10), which ideally necessitates an understanding of its underlying causative functional pathways. Towards this goal, the specific purpose of the present study was to explore a possible regulatory association between the transcription factor EGR-1 and the expression of PDGF-A, MIC-1, and FASN. Our primary focus was the analysis of this potential regulatory network by mining extensive data sets consisting of expression levels of EGR-1, PDGF-A, MIC-1, and FASN, in human prostate tissues. Findings from these analyses were corroborated by ectopic control of EGR-1 and its effect on PDGF-A, MIC-1, and FASN expression in the non-cancerous RWPE-1 human prostate epithelial cell model. Accordingly, our data indicates that the key transcription factor EGR-1 positively regulates PDGF-A and FASN, and negatively regulates MIC-1. These associations provide novel insight into pathways underlying prostate field effect, which

may lead to the development of targeted intervention strategies preventing progression from pre-malignancy to cancer.

Materials and Methods

Tissues

The tissue cohort utilized in the present study represents a combination of the cohorts reported in our previous studies on prostate field effect (12, 13). These tissues were collected in agreement with all Federal, State, and University laws, from consenting patients undergoing prostatectomy and donating approximately 100-500 mg of remnant tissue for molecular analyses. Individual cases of de-identified disease-free tissue samples were obtained from the Cooperative Human Tissue Network (CHTN) supported by the National Institutes of Health (NIH; located at Vanderbilt University, Nashville TN). All tissues were available as formalin fixed and paraffin embedded (FFPE) sections of 5 micrometer thickness (processed by the University of New Mexico Health Sciences Center, Department of Pathology or provided by CHTN). The study was approved by the Institutional Review Board of the University of New Mexico Health Sciences Center specifically approved the present study (#05-417). The combined tissue cohort consisted of 14 adenocarcinomas, 16 tumor adjacent tissues, and 9 disease-free tissues. 12 tumor adjacent and tumor tissues were matched; for the missing unmatched tissues, the quality of data was insufficient for inclusion into the final results. The definition of the term "tumor adjacent" in our studies refers to tissue resected at a distance of approximately 1 centimeter from the visible tumor margin. The definition of the term "disease-free" refers to prostate specimens from autopsy cases from individuals who died due to conditions unrelated to cancer. All tissues had been histologically reviewed previously by surgical pathologist E.G Fischer (University of New Mexico Health Sciences Center, Department of Pathology, Albuquerque NM), especially to exclude the presence of cryptic cancer cells in the tumor adjacent prostate tissues (12, 13). The mean age of all cases utilized was 56.1 years with a range of 26-79 years. The cancer specimens featured Gleason scores from 6 to 9 and pathological tumor node metastasis (TNM) stages (according to the American Joint Committee on Cancer; https://cancerstaging.org/Pages/default.aspx) from T2c to T3b (Table I).

Quantitative immunofluorescence

The generation of quantitative immunofluorescence data was reported in our previous studies on prostate field effect (12, 13). These procedures included deparaffinization, antigen retrieval, and immunostaining using specific primary antibodies and Alexa Fluor 633-conjugated secondary antibodies. For reference purposes, we list here the specific reagents, while the experimental details are described in (12, 13). The primary antibodies were: Anti-EGR-1 mouse monoclonal antibody ab54966 (at 3µg/ml) from Abcam (Cambridge MA); anti-MIC-1 goat polyclonal antibody ab39999 (at 3µg/ml) from Abcam (Cambridge MA); anti-PDGF-A rabbit polyclonal antibody sc-7958 (at 3µg/ml) from Santa Cruz Biotechnology (Santa Cruz CA); and anti-FASN rabbit polyclonal antibody sc20140 (H-300) (at 8µg/ml) from Santa Cruz Biotechnology (Santa Cruz CA). The corresponding control antibodies to ensure target specificity at the same concentrations were: Normal mouse IgG (GC270,

Millipore, Billerica MA), normal rabbit IgG (10500C, Invitrogen, Carlsbad CA), and normal goat IgG (10200, Invitrogen, Carlsbad CA). The corresponding secondary antibodies were Alexa Fluor 633 conjugated goat anti-mouse IgG, Alexa Fluor 633 conjugated goat anti-rabbit IgG, and Alexa Fluor conjugated rabbit anti-goat IgG (A21052, A21070, A21086, respectively; all from Invitrogen, Carlsbad CA). Nuclear counterstaining was performed with diamidino-2-phenylindole (DAPI).

Quantitative assessment of fluorescence was by spectral image acquisition and linear unmixing modes of confocal microscopy performed at the University of New Mexico Health Sciences Center Fluorescence Microscopy Shared Resource Core Facility as described previously by us (12, 13). Of note, control tissue slides with DAPI only, secondary antibody only, as well as unstained tissue were imaged separately to generate specific emission spectra for nuclear staining (DAPI; 405 nm excitation, 433 nm emission), Alexa Fluor (633 nm excitation, 490 nm emission), and background autofluorescence (ditto as per Alexa Fluor), respectively. These spectra were subjected to linear unmixing, a process that was equally applied to all spectral images to ensure the validity of inter-tissue comparisons. Consistent with our previous studies (12, 13), quantification was achieved by digital imaging of the spectrally unmixed confocal images using two data acquisition modes: (i) Whole image analysis: The total Alexa Fluor 633 signal was ratio-normalized to the total DAPI signal to account for number of cells and cell density per slide, which tends to be different between cancerous and non-cancerous tissues. For EGR-1, the whole image data acquisition mode was applied in three settings, i.e. whole cell (no selection), nuclear selection, and cytoplasmic selection, according to its ability to translocate between the two cell compartments (14). (ii) Region of interest (ROI) analysis: 3 representative ROI (defined as areas with robust immunostaining) per slide were chosen and the cumulative signal specific for Alexa Fluor 633 was determined. The ROI acquisition mode was applied to all factors according to their typical expression, i.e. both nuclear and cytoplasmic for EGR-1, extranuclear for MIC-1 and PDGF-A, and cytoplasmic for FASN. The size of ROI was identical from image to image (~80μm^2 each) and they were chosen by persons blinded to the nature of the tissue (Mrs. Virginia Severns, Ms. Fiona Bisoffi, Ms. Suzanne Jones) to avoid bias (shown in Fig. 1B). All original red signals were converted to yellow for better visibility. In total, 488 images with associated quantitative immunofluorescence data were available for the present analysis (Table I).

Computational transcription factor binding site analysis

Computational searches for potential transcription factor binding site were performed using the Tfsitescan software of the Molecular Informatics Resource for the Analysis of Gene Expression (MIRAGE) provided by the Institute for Transcriptional Informatics (IFTI) at http://www.ifti.org/cgi-bin/ifti/Tfsitescan.pl. Genomic sequences for EGR-1, PDGF-A, MIC-1, and FASN were retrieved from the GRCh38 Primary Assembly of the Gene database available at the National Center for Biotechnology Information (NCBI; http://www.ncbi.nlm.nih.gov/). The specific reference sequences and locations were: NC_000005.10, *Homo sapiens* chromosome 5, location 138,465,492-138,469,315 for EGR-1; NC_000019.10, *Homo sapiens*

chromosome 19, location 18,386,158-18,389,176 for MIC-1; NC_000007.14, *Homo sapiens* chromosome 7, location 497,258-520,123 for PDGF-A; and NC_000017.11, *Homo sapiens* chromosome 17, location 82,078,338-82,098,230 for FASN. The genomic sequences were subjected to searches for the EGR-1 recognition sequence (GCG(G/T)GGCG) (15).

Cell culture and transfections

Non-cancerous RWPE-1 human prostate epithelial cells were purchased from the American Type Culture Collection, Manassas VA and cultured in serum-free keratinocyte basal medium containing 4500mg/L glucose, 0.05mg/ml bovine pituitary extract and 5 ng/ml recombinant epidermal growth factor (Invitrogen, Carlsbad CA). Cells were maintained at 37°C in a humidified 5% CO_2 atmosphere. Trypsin-EDTA at 0.25% was used to detach the cells for splitting and re-culturing. pcDNA3.1 control and pcDNA3.1/EGR-1 plasmids were a kind gift of Dr. W. Xiao, University of Science and Technology of China, Hefei, China. pLKO.1 control and pLKO.1/EGR-1 shRNA plasmids were from Sigma St. Louis MO. Plasmids were propagated in *E. coli* strain JM109 grown in LB broth containing 100ug/mL ampicillin and purified using spin column chromatography (Qiagen, Valencia CA). Transfections were performed with 1µg plasmid DNA in 24-well plates containing 150,000 cells per well using Lipofectamine 2000 reagent (Invitrogen, Carlsbad CA) and for 48 hours. Our transfection protocol yields reproducible transfection rates of 45±5% for pairs of empty control and cDNA carrying plasmids (fluorescence based assay, not shown). Cells were snap frozen in liquid nitrogen to preserve RNA integrity and stored short term at -80˚C.

Quantitative Reverse Transcriptase Polymerase Chain Reaction (qRT-PCR) and Western blotting

RNA was isolated using spin column chromatography (Qiagen, Valencia CA). 1-3µg of RNA were transcribed to cDNA using random decamers of the Retroscript™ RT Kit (Life Technologies, Carlsbad CA). mRNA expression was quantitated in a CFX Connect Real Time PCR Detection System from Bio-Rad (Hercules CA) using the SYBR Green PCR Master Mix and SYBR Green RT-PCR Reagents Kit (Life Technologies, Carlsbad CA) in 25ul reactions, using 100ng of template cDNA and a final primer concentration of 900nM. The cycling parameters were 95˚C for 5 minutes followed by 45 cycles of 94˚C for 15 seconds, and 51-58˚C for 1 minute. Primers were designed using Primer Express software (Invitrogen, Carlsbad CA) and synthesized by Integrated DNA Technologies (Coralville IA). The following primer sequences (5'to 3') were used: EGR-1 forward: GAGCAGCCCTACGAGCAC; EGR-1 reverse: AGCGGCCAGTATAGGTGATG; MIC-1 forward: CTACAATCCCATGGTGCTCAT; MIC-1 reverse: TCATATGCAGTGGCAGTCTTT; PDGF-A forward: CGTAGGGAGTGAGGATTCTTT; PDGF-A reverse: GCTTCCTCGATGCTTCTCTT; FASN forward: AGAACTTGCAGGAGTTCTGGGACA; FASN reverse: TCCGAAGAAGGAGGCATCAAACCT; TATA Binding Protein (TBP) forward: CACGAACCACGGCACTGATT; TBP reverse: TTTTCTTGCTGCCAGTCTGGAC. qRT-PCR reactions were performed in triplicate. Relative expression levels

were determined by the ΔΔCt method using TBP as normalization control after determining that amplification efficiencies were similar to the ones of the control transcripts.

Protein lysates were generated on ice in lysis buffer: 25 mM Tris, 8 mM $MgCl_2$, 1 mM DTT, 15% glycerol, 1% TritonX-100, protease inhibitor cocktail (Sigma St. Louis MO). Insoluble cell material was removed by centrifugation of lysates at 13,000 rpm for 10 min at 4°C. The protein concentration was determined by Bradford assay (Sigma St. Louis MO) against a bovine serum albumin (BSA) standard. 80 µg total protein were size-separated by sodium dodecyl sulfate polyacrylamide gel electrophoresis (SDS-PAGE), electro-blotted onto polyvinylidene (PVDF) membranes, blocked with 5% milk powder in Tris buffered saline, and probed overnight with anti-EGR-1 and anti-β-actin primary antibodies (sc-189 from Santa Cruz Biotechnology, Dallas TX and A1978 from Sigma St. Louis MO, respectively). Detection and chemiluminescent visualization (Clarity ECL Substrate, BioRad, Hercules CA) of EGR-1 and β-actin was performed using host-matched secondary horseradish peroxidase-conjugated antibodies (Sigma St. Louis MO). The quantitative signal intensity of bands was determined by densitometry using ImageJ software (https://imagej.nih.gov/ij/).

Statistics

EGR-1, PDGF-A, MIC-1, and FASN expression levels were represented by signal intensities (sum pixel count per area) generated by quantitative immunofluorescence analysis (as described above). Straightforward, yet robust statistical methods were applied to the data sets using the Microsoft Office Excel software package (Redmond WA). The data sets were inclusive (all available informative images), for matched cases only, or separated by the means. These approaches are indicated in the Results section.

Correlations between the expression of EGR-1 and PDGF-A, MIC-1, and FASN were analyzed by several statistical methods. To control for small sample size and a distribution with infinite variance due to tissue heterogeneity (expressed as coefficient of variation in %; reported in the text of Results), the Wilcoxon rank sums test (as opposed to the Student t-test) was used for pairs of data sets (reported in the text of Results). The single factor Analysis of Variance (ANOVA) was applied for comparisons of multiple data sets with unequal variances. Statistical significance for the change of ratios of PDGF-A, MIC-1, or FASN to EGR-1 in tumor adjacent and tumor tissues as compared to disease-free tissues was determined by the two-tailed Student t-test (statistical significance defined as $p \leq 0.05$; reported in Fig. 2A and 2B). The data sets were further mined for potential associations between factors by determining the Pearson correlation coefficient r. The significance for these observations was determined by first calculating the t-value of the correlation using the equation t=r/SQRT(1-r^2/n-2), where r is the correlation coefficient, n is the number of samples, and 2 is the degree of freedom. The t-value was then used to determine the significance of r by the two-tailed Student's t distribution (TDIST; statistical significance defined as $p \leq 0.05$; reported in the text, but not shown). Statistical significance for the change of ratios of positive to negative Pearson correlations of PDGF-A, MIC-1, and FASN to EGR-1 in tumor adjacent

and tumor tissues as compared to disease-free tissues was determined by the f-test with a p value of ≤ 0.05 considered to be significant (reported in Fig. 3B and 3D).

Results

Immunofluorescence detection of EGR-1, PDGF-A, MIC-1, and FASN in human prostate tissues

We previously reported on the extent of individual expression of EGR-1, PDGF-A, MIC-1, and FASN to support the concept of field effect in histologically normal prostate tissues adjacent to histologically overt adenocarcinomas, as compared to disease-free tissues (12, 13). To begin unraveling the functional pathways of field effect in prostate tissues, here we analyzed the potential association between these markers of field effect in human prostate tissues of different histology. For this analysis, a total of 488 digitized images from 39 individual human prostate tissue samples were available for a comprehensive analysis (Table I). The images indicate the specific detection of EGR-1, PDGF-A, MIC-1, and FASN by immunofluorescence which was quantified computationally (12, 13). Representative images are shown in Fig. 1A. In general, the expression of EGR-1, PDGF-A, MIC-1, and FASN was highest in tumor and lowest or absent in disease-free tissues (Fig. 1A i-iv and 1A ix-xii, respectively). Furthermore, tumor adjacent tissues tended to display elevated expressions of all factors (Fig. 1A v-viii). The specificity of detection was corroborated by the absent staining with isotype specific control antibodies (Fig. 1A xiii-xv).

Quantification and association analyses of EGR-1, PDGF-A, MIC-1, and FASN expression in human prostate tissues

We have previously developed sensitive quantification methods for signals generated by immunofluorescence in human prostate tissues ((12, 13) and Methods). These methods include whole image and region of interest data acquisition modalities for all investigated factors (see Materials and Methods). Furthermore, in line with the aim of this study to be as comprehensive as possible with respect to associative analyses, EGR-1 expression was measured using three specific settings for cell compartmentalization: Whole cell, as well as nuclear and cytoplasmic separately. This is supported by an elegant study by Mora et al (14) who showed that EGR-1 can shuttle between these locations depending on cellular type and context. These different types of data acquisition is shown in (Fig. 1B).

While our previous reports compared the level of expression for EGR-1, PDGF-A, MIC-1, and FASN in disease-free, tumor adjacent, and tumor tissues, thereby supporting the concept of field effect (12, 13), the primary objective of the present work was to explore a potential relationship between these factors and to determine whether that relationship changes in different types of tissues. As expected, and typical for human tissue studies, both the whole image and the region of interest data acquisition modes resulted in substantial heterogeneity with respect to variation of expression of all factors in disease-free, tumor adjacent, and tumor tissues. The coefficient of variations ranged from 4.7% to 39.0% in the whole image and from 3.9% to 31.1% in the region of interest measurements.

Quantified expression data was comprehensively analyzed for similarities, discrepancies, and associations using straightforward, yet robust statistical methods. Of note, because of the expected inter- and intra-tissue heterogeneity, the identification of outliers was not meaningful and we adopted an inclusive approach in which we did not exclude any data points. In addition, due to different antibody affinities for their targets, we determined that comparisons of the mean, variance, and distribution of expression data between factors would not be good indicators of a causative regulatory role of EGR-1 for the other factors. In fact, group analysis by ANOVA indicated that all expression patterns in all types of tissues were distinct from each other ($p<0.001$), and individual comparisons by Wilcoxon rank sum test were non-informative with respect to the distinction between induction and repression ($p \leq 0.05$) or coupled expression ($p > 0.05$). Consequently, we chose to analyze the change of the ratio of either PDGF-A, MIC-1, or FASN to EGR-1 in disease-free compared to tumor adjacent and tumor tissues. Based on our previous results showing that prostate tissues adjacent to adenocarcinomas feature a field effect compared to disease-free tissues (12, 13), such a change in ratio would suggest a potential regulatory role of EGR-1 in agreement with its proven up-regulation during tumorigenesis and cancer progression (16). Accordingly, EGR-1 expression determined by both the whole image and region of interest acquisition modes in all available tissues revealed an increase of all factors-to-EGR-1 ratios, up to 2.5-fold for PDGF-A, 16.9-fold for MIC-1, and 2.8-fold for FASN (Fig. 2A and 2B, left bar graphs). Similarly, when analyzed for matched adjacent and tumor tissues only (derived from the same patients, respectively), the ratio of the other factors to EGR-1 in both acquisition modes markedly increased, up to 136.4-fold for PDGF-A, 273.8-fold for MIC-1, and 2.5-fold for FASN (Fig. 2A and 2B, right bar graphs). While this analysis does not reveal the direction of regulation (positive or negative), the changes do indicate a regulatory function of EGR-1 for PDGF-A, MIC-1, and to a lesser extent for FASN.

The changes in expression ratio of PDGF-A, MIC-1, and to some extent FASN, prompted us to refine our determination of a potential regulatory effect of EGR-1 on these factors by using Pearson's correlation analysis, which is independent of differences in antibody affinities for the different factors. By definition, this approach included tissues from matched cases only. To refine our analysis, we also separated all expression data by the median and determined the correlation between expression levels above and below median values. Similar to the ratio analysis described in Fig. 2, we attempted to corroborate possible regulatory effects of EGR-1 for PDGF-A, MIC-1, and FASN expression by comparing Pearson's correlations between different types of tissues, i.e. disease-free, tumor adjacent, and tumor tissues. Fig. 3A and 3C show a graphical representation of all possible correlations between whole cell, nuclear, and cytoplasmic EGR-1 and PDGF-A, MIC-1, and FASN expression in disease-free, tumor adjacent, and tumor tissues as acquired by whole image and region of interest acquisition mode, respectively. In contrast to group analyses by ANOVA or individual comparisons by Wilcoxon rank sum test, Pearson's correlation analyses are indicators of positive vs. negative regulation. The significance (average p) of the Pearson's correlation coefficients for the whole image acquisition mode was 0.16, 0.24, and 0.25 (with 40%, 7%, and 18% of all coefficients being $p \leq 0.05$) for PDGF-A, MIC-1, and FASN, respectively. For the region of

interest acquisition mode, the significance (average p) for the corresponding factors was 0.21, 0.21, and 0.25 (with 17%, 23%, and 7% of all coefficients being $p \leq 0.05$). Visual inspection of the Pearson's correlation analyses in Fig. 3A and 3C indicates that EGR-1 positively and negatively regulates PDGF-A and MIC-1, respectively, while the results for FASN regulation were less clear due to the contrasting data between the two data acquisition modes. Similar to the ratio analysis described in Fig. 2, we attempted to corroborate possible regulatory effects of EGR-1 for PDGF-A, MIC-1, and FASN expression by comparing Pearson's correlations between different types of tissues, i.e. disease-free, tumor adjacent, and tumor tissues. Given the high tissue heterogeneity, we used an inclusive approach and compared the average of all positive and negative correlations ($r > 0$ or $r < 0$) for each factor in the three types of tissue. This analysis showed a progressive positive and negative regulation of PDGF-A (up to 64.6-fold) and MIC-1 (up to 10-fold), respectively in tumor adjacent and tumor compared to disease-free tissues. Again, results for FASN were less clear with contrasting results depending on the data acquisition mode (Fig. 3B and 3D). These possible regulations were confirmed by visually linking the means of Pearson's correlations in the different types of tissues (Fig. 3A and 3B).

Computational and cell experimental analysis of EGR-1 regulation of PDGF-A, MIC-1, and FASN

The theoretical potential of the transcription factor EGR-1 to be a regulator of PDGF-A, MIC-1, and FASN expression was determined computationally using Tfsitescan software applied to 1500 base pairs upstream and 500 base pairs downstream of the transcription initiation site on the genomic sequences of PDGF-A, MIC-1, and FASN. Thus, a total of 2000 base pairs were screened for the presence of the EGR-1 recognition sequence (GCG(G/T)GGCG) (15). This analysis resulted in the identification of two, one, and four recognition sequences for PDGF-A, MIC-1, and FASN, respectively (Fig. 4A). Regulation of PDGF-A, MIC-1, and FASN expression by EGR-1 was experimentally tested by over-expression and suppression of EGR-1 in transient transfection experiments using the non-cancerous RWPE-1 human prostate epithelial cell model. The immortalized but non-cancerous RWPE-1 cells were chosen because they best represent the tissues analyzed in this study, which are almost exclusively early stage malignancy and tumor adjacent, i.e. best reflective of field effect. Transfections with the pcDNA3.1 and the pLKO.1 plasmids typically resulted in 50-100-fold over-expression and suppression of EGR-1 at the mRNA level (not shown). Modulation of EGR-1 protein expression was verified by Western blotting and resulted in approximately 2-fold over-expression and suppression. Although the regulatory effects on PDGF-A, MIC-1, and FASN were rather small, transient EGR-1 over-expression up-regulated PDGF-A and FASN protein expression (up to 2-fold) and down-regulated MIC-1 protein expression (up to 3-fold), while transient EGR-1 suppression corroborated this effect by up-regulating MIC-1 protein expression (approximately 1.5-fold), while down-regulating PDGF-A and FASN protein expression (up to 2-fold)(Fig. 4B). These results were accompanied by similar changes at the mRNA level, as measured by qRT-PCR. Accordingly, transient EGR-1 over-expression up-regulated PDGF-A and FASN (up to 2-fold) and down-regulated MIC-1 (up to 2-fold), while transient EGR-1 suppression corroborated this effect by down-regulating PDGF-A and FASN (up to

2.5-fold and 5-fold, respectively) and by up-regulating MIC-1 (up to 10-fold)(Fig. 4C). Overall, these results are in good agreement with the observations made in the tissues.

Discussion

The importance of field effect, or field cancerization, in the prostate has been well recognized as worthy of being explored in detail for the benefit of developing clinical applications towards a better clinical management of prostate cancer (8-10, 17). For example, we have previously argued that prostate field effect could be used to improve the diagnosis of prostate cancer in false negative biopsies (10). The latter remains an important and continuous challenge in confirmatory diagnosis of prostate adenocarcinoma that has clinical, psychological, and financial implications (18-21). Accordingly, field cancerized tissue could increase the clinically informative area that can be analyzed microscopically by a surgical pathologist if histology could be combined with immunological techniques. In this scenario, the pathologist would recognize the presence and location of a lesion even in the absence of its visual confirmation thereby avoiding false negative calls, even after repeated biopsies (22). This possibility has prompted others to term tissues affected by field effect "TINT" (for "tumor indicating normal tissue"; (8)). Even in the case of a positive identification of cancer, the extent (number of positive biopsy cores, % of tissue affected) and the grade (Gleason) may indicate low-risk for progression and thus eligibility for active surveillance with frequent testing for serum prostate specific antigen (PSA), as opposed to prostatectomy (23). It is conceivable that during active surveillance, a recognized field effect could be monitored and queried as an indicator of potential progression (10, 24). This would help mitigate the well-known overtreatment of prostate cancer with surgery, which albeit performed with curative intent, may unnecessarily decrease quality of life due to its severe side effects (25, 26). The latter approach could also be amenable to the assessment of pre-surgical neo-adjuvant therapeutic interventions, for which the efficacy could be monitored during active surveillance by established markers and parameters of field effect (10, 27). A further potential application of field effect lies in its inclusion in the definition of surgical margins for focal therapy, which seems to be on the rise as a form of less invasive therapy and as more refined interventions have developed (10, 28, 29). As such, the presence of a field effect at the margin may be indicative of elevated risk for progression or of the extent of tumor multifocality within the prostate (10, 30). Of note, the common assumption underlying the afore-mentioned potential applications of prostate field effect is that a field exists as a consequence of the presence of a lesion. However, it is also conceivable that field effect precedes tumor formation and represents a truly pre-malignant status evident at the molecular level but in absence of any histological change. In fact, the latter view is widely accepted (8-10, 17) and defines field cancerized prostate tissues as a temporal record of tumorigenesis. As such, it is a source for early biomarkers and potential targets for preventative strategies (8, 10).

Pertinent to all applications of field effect is the knowledge of the molecular markers and pathways that are characteristic for it. We and others have previously compiled lists of molecular markers reported in the scientific literature (7-10), but for most of these factors the etiology remains unknown. For markers of field effect to be of best use, either as indicators or as targets, it is important to begin identifying distinct cellular and molecular events

and pathways that underlie the formation of a field. Towards this goal, in this report we have established a link between four protein factors of prostate field effect, which were originally identified individually or deduced from the literature. We had identified the key transcription factor EGR-1, the divergent member of the transforming growth factor β (TGF-β) MIC-1, and the lipogenic oncogene FASN as being elevated in prostate tissues 1 centimeter from the visible tumor margin (11). While our original work was microarray-based and thus RNA specific, we subsequently confirmed EGR-1, MIC-1, FASN, and PDGF-A protein up-regulation in field cancerized human prostate tissues (12, 13).

EGR-1 is a central regulator of many molecular pathways and acts divergently according to cell context (31). While in other types of tissues, it may function primarily as a tumor suppressor, it ultimately assumes, with some ambiguity, a tumor promoting role in prostate cancer development and progression (16, 32, 33). The role of the secreted factor PDGF-A in prostate cancer is well established. It is one of four isoforms that binds as a dimer to the tyrosine kinase receptors PDGFRα and PDGFRβ. PDGF-A stimulates growth, survival, and motility of various cell types and when hyperactivated, promotes prostate cancer development and progression through paracrine and autocrine actions (34, 35). Equally established in prostate cancer development and progression is FASN, which has been termed a metabolic oncogene and is the target of ongoing efforts to develop specific inhibitors of its lipogenic activity promoting tumor cell proliferation through lipid biosynthesis and posttranslational protein modification (36, 37). The role of MIC-1 is less clear and is reported as both a cancer promoter and suppressor (38, 39). Originally discovered in macrophages (40), it may promote a pro-tumorigenic environment when secreted by prostate cancer cells by suppressing the anti-cancer activity of immune cells (41).

It is conceivable that the concerted actions of MIC-1, PDGF-A, and FASN can lead to the formation of molecularly altered fields through autocrine stimulation of hyperproliferative cell foci prone to further genetic and biochemical change towards transformation, which is congruent with the definition of a pre-malignant field effect. However, the possibility of cross-regulatory influences of these actions remain unknown. Since EGR-1 is a pleiotropic transcription factor, we hypothesized that it could regulate MIC-1, PDGF-A, and FASN. The present work aimed at testing this possibility through comprehensive association analyses using quantitative immunofluorescence expression data generated in human prostate tissues. EGR-1 has previously been shown to induce many target genes, including PDGF-A in the LAPC4 cell model of prostate cancer after ectopic over-expression of EGR-1 (42). Similarly, MIC-1 seems to be positively regulated by EGR-1 in the LNCaP prostate cancer cell model (43). In contrast, there is a lack of information for a potential regulatory function of EGR-1 for FASN in prostate cells or tissues, although our computational analysis of genomic DNA upstream and downstream of the transcription initiation site indicates multiple EGR-1 recognition sequences. Our own ectopic EGR-1 over-expression and suppression data in RWPE-1 cells confirms a positive regulation of PDGF-A, but resulted in a negative regulation of MIC-1. An obvious reason for this discrepancy is that RWPE-1 represents a non-cancerous pre-malignant, as opposed to an advanced cancer cell model, such as LNCaP (43). At the experimental level, the use of reporter constructs for MIC-1 activity (43) *vs.* qRT-PCR using specific primers

may also have contributed to differences in the result. More importantly however, our *in vitro* findings are supported by our extensive *in situ* association studies in human tissues which are based on factor correlations and their changes from disease-free to tumor adjacent to cancerous tissues, thereby confirming the presence of a field effect. With respect to PDGF-A, our data shows a positive association with EGR-1 which supports a positive regulation. Using two data acquisition modes, our results suggest a negative regulation of EGR-1 for MIC-1, which is in accordance with our observations in RWPE-1 cells. Finally, FASN expression levels were positively associated with EGR-1 expression, which was in agreement with tissues expression data acquired in whole image mode.

In summary, three principal conclusions can be drawn from our findings. First, immunohistochemistry and immunofluorescence are techniques usually employed towards qualitative assessment of protein expression and localization in cells and tissues in a static manner. However, we show here that using sophisticated quantitation methods, such as spectral image acquisition, linear unmixing, and digital imaging developed in our previous reports (12, 13), can deliver meaningful indications of molecular associations in a physiologically relevant in *situ* environment, even in the presence of high heterogeneity. A related issue is the use of ROIs in quantitation. ROIs are often used to compensate for inequalities of cell composition. Although our data shows good congruency between the whole image and ROI approaches for the most part, it also cautions for care with respect to the number of ROIs and their random and blinded placement. Second, our study prompts for caution when comparing molecular association data generated in cell models with data stemming from tissues. Although it can be argued that tissue studies are static and compromised by sample heterogeneity, they can provide meaningful indications of molecular regulations when coupled with sophisticated data acquisition. Also, tissues are physiologically relevant, better reflect the complexity of cellular and molecular pathways influenced by the environment, and can guide confirmatory studies in cell models. Third, we propose EGR-1 to be a key regulator of prostate field effect through induction of pro-proliferative and pro-metabolic (PDGF-A and FASN, respectively) and suppression of pro-apoptotic (MIC-1) factors. This is supported in particular by our comparative data between disease-free and tumor adjacent tissues (field effect). Admittedly, while the positive regulation of PDGF-A and FASN by EGR-1 can be easily acknowledged, its regulatory function for MIC-1 seems less clear due to its concomitant up-regulation in tumor adjacent tissues (13). However, it is important to note that these findings are not in disagreement, as MIC-1 regulation has been discussed to be complex (38, 39). This may be reflected in a complex *in situ* environment, such as tissues, where many other factors may also exert their regulatory effect. Future studies are warranted to test the exact mechanisms of direct and/or indirect regulation under physiological conditions, such as in animal models. Because it is widely accepted that field effect represents a pre-malignant state, such knowledge may help develop targeted intervention strategies preventing progression to cancer.

Acknowledgements

We thank the following individuals at the New Mexico Health Sciences Center, Department of Pathology and Hospital: Trisha Fleet for procuring prostate tissues through patient consent; Myra Zucker, Cathy Martinez, and Kari Rigg for skillfully preparing prostate tissue sections; surgical pathologist Dr. E.G Fischer for histological review of all prostate tissues utilized in this study. We acknowledge Kerry Wiles from the Cooperative Human Tissue Network (CHTN; Western Division, Nashville TN) for the successful procurement of prostate tissues and annotated reports. We are grateful to Genevieve Phillips and Dr. Rebecca Lee from the University of New Mexico & Cancer Center Fluorescence Microscopy Shared Resource for excellence assistance and technical input for generating the images by spectral imaging and linear unmixing. We thank Ms. Virginia Severns, Ms. Fiona Bisoffi, and Ms. Suzanne Jones for the unbiased placing of the region of interest boxes for signal quantitation in the tissue images. The departmental offices and staff of the University of New Mexico, Department of Biochemistry and Molecular Biology, the University of New Mexico, Office of Medical Student Affairs, and the Chapman University Schmid College of Science and Technology are acknowledged for administrative support. This work was supported by National Institutes of Health (NIH) Grant RR0164880, NIH Grant R03CA136030-02, and Department of Defense Prostate Cancer Research Program grant W81XWH-15-1-0056 (to M. Bisoffi), University of New Mexico Cancer Center Support Grant NIH/NCI P30CA118110, grants from the Chapman University Office of Undergraduate Research program (to K. Gabriel and E. Frisch), and a generous gift from Melinda and Edward Subia of Orange County CA.

Figure Legends

Figure 1

(A) Representative detection of EGR-1, PDGF-A, MIC-1, and FASN by immunofluorescence in tumor (i-iv), tumor adjacent (v-viii), and disease-free (ix-xii) human prostate tissues. Unspecific IgG of mouse, rabbit, and goat origin were tested for absence of staining (xiii-xv). Images represent Alexa Fluor 633 immunostaining (yellow signals); the smaller insets represent corresponding nuclear staining by DAPI (blue); white bars represent 10μm. (B) Schematic representation of the whole image (top) and region of interest (bottom) quantitative acquisition modes for EGR-1 fluorescence intensity. Whole image data acquisition includes three different settings as defined by DAPI staining, whole cell/no selection (i), nuclear (ii), and cytoplasmic (iii) as indicated by the bright blue shading. Region of interest data acquisition includes nuclear (iv) and extranuclear/cytoplasmic (v) as indicated by the areas designated by the randomly placed yellow rectangle frames (~80μm^2); white bars represent 10μm.

Figure 2

(A) and (B) Ratios of PDGF-A, MIC-1, and FASN to EGR-1 expression (combined wc, nu, cy) in disease-free (DF), tumor adjacent (ADJ), and tumor (TUM) tissues using images from all (left three bars) and matched only (right three bars) cases, acquired by the whole image and the region of interest mode, respectively. The bars represent average ratios + standard errors. The numbers by the bars represent the fold change in ADJ and TUM compared to DF tissues. Asterisks denote statistical significance compared to DF tissues ($p \leq 0.05$).

Figure 3

(A) and (C) Graphical representation of Pearson's correlations (*r*) between EGR-1 and PDGF-A, MIC-1, and FASN using data from digitized images acquired by the whole image and the region of interest mode, respectively. Within each type of tissue, disease-free (DF), tumor adjacent (ADJ), and tumor (TUM), correlations were determined for all matched, and for EGR-1 above or below the median with the corresponding median-divided data sets of PDGF-A, MIC-1, and FASN. Data sets in A consist of whole cell, nuclear, and cytoplasmic EGR-1 measurements (total of 15 correlations per factor); data sets in B consist of nuclear and cytoplasmic EGR-1 measurements (total of 12 correlations per factor). Arrows depict the change of regulation by linking the mean Pearson's correlations (black dots) in the different types of tissues. (B) and (D) Average positive (pos; black bars) and negative (neg; grey bars) Pearson's correlations (*r*) between EGR-1 and PDGF-A, MIC-1, and FASN in DF, ADJ, and TUM tissues acquired by the whole image and the region of interest mode, respectively. The bars represent average ratios + standard errors. The numbers represent the fold change in the ratio of positive/negative *r* in ADJ and TUM compared to DF tissues. Asterisks denote statistical significance compared to DF tissues ($p \leq 0.05$).

Figure 4

(A) Computational analysis of the EGR-1 recognition sequence (GCG(G/T)GGCG) in the genomic sequence 1500 base pairs upstream and 500 base pairs downstream of the transcription initiation site of PDGF-A, MIC-1, and FASN. Black vertical lines and black rectangular boxes denote genomic sequences and exons, respectively; vertical arrow heads indicate EGR-1 recognition sequences. (B) EGR-1, PDGF-A, MIC-1, and FASN protein expression in RWPE-1 cells transiently transfected with pcDNA3.1/EGR-1 (EGR-1 over-expression) or pLKO.1/EGR-1 shRNA (EGR-1 suppression), and their empty plasmid controls. Double bands in EGR-1 represent post-translational modifications as per (44). The fold change difference compared to empty plasmid control and determined by densitometry as a ratio with β-actin signal is indicated in the small bar graphs (left bar = EGR-1 over-expression; right bar = EGR-1 suppression). (C) Relative mRNA expression of PDGF-A, MIC-1, and FASN in RWPE-1 cells transiently transfected with pcDNA3.1/EGR-1 (EGR-1 over-expression) or pLKO.1/EGR-1 shRNA (EGR-1 suppression), and their empty plasmid controls. Bars represent averages of triplicates ± standard deviation; * denotes statistical significance ($p \leq 0.05$) from pcDNA3.1 and pLKO.1 plasmid vector control, respectively.

References

1. Epstein JI: Mimickers of prostatic intraepithelial neoplasia. Int J Surg Pathol 18: 142S-148S, 2010.
2. Montironi R, Mazzucchelli R, Algaba F and Lopez-Beltran A: Morphological identification of the patterns of prostatic intraepithelial neoplasia and their importance. J Clin Pathol 53: 655-665, 2000.
3. De Marzo AM, Platz EA, Sutcliffe S, Xu J, Gronberg H, Drake CG, Nakai Y, Isaacs WB and Nelson WG: Inflammation in prostate carcinogenesis. Nat Rev Cancer 7: 256-269, 2007.
4. De Marzo AM, Marchi VL, Epstein JI and Nelson WG: Proliferative inflammatory atrophy of the prostate: implications for prostatic carcinogenesis. Am J Pathol 155: 1985-1992, 1999.
5. Slaughter DP, Southwick HW and Smejkal W: Field cancerization in oral stratified squamous epithelium; clinical implications of multicentric origin. Cancer 6: 963-968, 1953.
6. Braakhuis BJ, Tabor MP, Kummer JA, Leemans CR ans Brakenhoff RH: A genetic explanation of Slaughter's concept of field cancerization: evidence and clinical implications. Cancer Res 63: 1727-1730, 2003.
7. Dakubo GD, Jakupciak JP, Birch-Machin MA and Parr RL: Clinical implications and utility of field cancerization. Cancer Cell Int 7: 2, 2007.
8. Halin S, Hammarsten P, Adamo H, Wilkstrom P and Bergh A: Tumor indicating normal tissue could be a new source of diagnostic and prognostic markers for prostate cancer. Expert Opinion in Medical Diagnostics 5: 37-47, 2011.
9. Nonn L, Ananthanarayanan V and Gann PH: Evidence for field cancerization of the prostate. Prostate 69: 1470-9. 2009.
10. Trujillo KA, Jones AC, Griffith JK and Bisoffi M: Markers of field cancerization: proposed clinical applications in prostate biopsies. Prostate Cancer 2012: 302894, 2012.
11. Haaland CM, Heaphy CM, Butler KS, Fischer EG, Griffith JK and Bisoffi M: Differential gene expression in tumor adjacent histologically normal prostatic tissue indicates field cancerization. Int J Oncol 35: 537-546, 2009.
12. Jones AC, Antillon KS, Jenkins SM, Janos SN, Overton HN, Shoshan DS, Fischer EG, Trujillo KA and Bisoffi M: Prostate Field Cancerization: Deregulated Expression of Macrophage Inhibitory Cytokine 1 (MIC-1) and Platelet Derived Growth Factor A (PDGF-A) in Tumor Adjacent Tissue. PLoS One 10: e0119314, 2015.
13. Jones AC, Trujillo KA, Phillips GK, Fleet TM, Murton JK, Severns V, Shah SK, Davis MS, Amith AY, Griffith JK, *et al*: Early growth response 1 and fatty acid synthase expression is altered in tumor adjacent prostate tissue and indicates field cancerization. Prostate 72: 1159-1170, 2012.
14. Mora GR, Olivier KR, Cheville JC, Mitchell RF, Jr., Lingle WL and Tindall DJ: The cytoskeleton differentially localizes the early growth response gene-1 protein in cancer and benign cells of the prostate. Mol Cancer Res 2: 115-128, 2004.

15. Pagel JI and Deindl E: Disease progression mediated by egr-1 associated signaling in response to oxidative stress. Int J Mol Sci 13: 13104-13117, 2012.
16. Gitenay D and Baron VT: Is EGR1 a potential target for prostate cancer therapy? Future Oncol 5: 993-1003, 2009.
17. Walia G, Pienta KJ, Simons JW and Soule HR: The 19th annual prostate cancer foundation scientific retreat. Cancer Res 73: 4988-4991, 2013.
18. Delongchamps NB and Haas GP: Saturation biopsies for prostate cancer: current uses and future prospects. Nat Rev Urol 6: 645-652, 2009.
19. Eichler K, Hempel S, Wilby J, Myers L, Bachmann LM and Kleijnen J: Diagnostic value of systematic biopsy methods in the investigation of prostate cancer: a systematic review. J Urol 175: 1605-1612, 2006.
20. Presti JC, Jr.: Prostate biopsy strategies. Nat Clin Pract Urol 4: 505-511, 2007.
21. Rabbani F, Stroumbakis N, Kava BR, Cookson MS and Fair WR: Incidence and clinical significance of false-negative sextant prostate biopsies. J Urol 159: 1247-1250, 1998.
22. Patel AR and Jones JS: Optimal biopsy strategies for the diagnosis and staging of prostate cancer. Curr Opin Urol 19: 232-237, 2009.
23. Pomerantz M: Active Surveillance: Pathologic and Clinical Variables Associated with Outcome. Surg Pathol Clin 8: 581-585, 2015.
24. Mazzucchelli R, Galosi AB, Santoni M, Lopez-Beltran A, Scarpelli M, Cheng L and Montironi R: Role of the pathologist in active surveillance for prostate cancer. Anal Quant Cytopathol Histpathol 37: 65-68, 2015.
25. Bellardita L, Valdagni R, van den Bergh R, Randsdorp H, Repetto C, Venderbos LD, Lane JA and Krfage IJ: How does active surveillance for prostate cancer affect quality of life? A systematic review. Eur Urol 67: 637-645, 2015.
26. Kwon O and Hong S: Active surveillance and surgery in localized prostate cancer. Minerva Urol Nefrol 66: 175-187, 2014.
27. Lou DY and Fong L: Neoadjuvant therapy for localized prostate cancer: Examining mechanism of action and efficacy within the tumor. Urol Oncol 34: 182-192, 2016.
28. Lindner U, Lawrentschuk N, Schatloff O, Trachtenberg J and Lindner A: Evolution from active surveillance to focal therapy in the management of prostate cancer. Future Oncol 7: 775-787, 2011.
29. Marshall S and Taneja S: Focal therapy for prostate cancer: The current status. Prostate Int 3: 35-41, 2015.
30. Andreoiu M and Cheng L: Multifocal prostate cancer: biologic, prognostic, and therapeutic implications. Hum Pathol 41: 781-793, 2010.
31. Pagel JI and Deindl E: Early growth response 1--a transcription factor in the crossfire of signal transduction cascades. Indian J Biochem Biophys 48: 226-235, 2011.
32. Adamson E, de Belle I, Mittal S, Wang Y, Hayakawa J, Korkmaz K, O'Hagan D, McClelland M and Mercola D: Egr1 signaling in prostate cancer. Cancer Biol Ther 2: 617-622, 2003.

33. Adamson ED and Mercola D: Egr1 transcription factor: multiple roles in prostate tumor cell growth and survival. Tumour Biol 23: 93-102, 2002.
34. Heldin CH: Autocrine PDGF stimulation in malignancies. Ups J Med Sci 117: 83-91, 2012.
35. Heldin CH: Targeting the PDGF signaling pathway in tumor treatment. Cell Commun Signal 11: 97, 2003.
36. Baron A, Migita T, Tang D and Loda M: Fatty acid synthase: a metabolic oncogene in prostate cancer? J Cell Biochem 91: 47-53, 2004.
37. Zadra G, Photopoulos C and Loda M: The fat side of prostate cancer. Biochim Biophys Acta 1831: 1518-1532, 2013.
38. Husaini Y, Qiu MR, Lockwood GP, Luo XW, Shang P, Kuffner T, Tsai VW, Jiang L, Russell PJ, Brown DA, *et al*: Macrophage inhibitory cytokine-1 (MIC-1/GDF15) slows cancer development but increases metastases in TRAMP prostate cancer prone mice. PLoS One 7: e43833, 2012.
39. Vanhara P, Hampl A, Kozubik A and Soucek K: Growth/differentiation factor-15: prostate cancer suppressor or promoter? Prostate Cancer Prostatic Dis 15: 320-328, 2012.
40. Bootcov MR, Bauskin AR, Valenzuela SM, Moore AG, Bansal M, He XY, Zhang HP, Donnellan M, Mahler S, Pryor K, *et al*: MIC-1, a novel macrophage inhibitory cytokine, is a divergent member of the TGF-beta superfamily. Proc Natl Acad Sci U S A 94: 11514-11519, 1997.
41. Karan D, Holzbeierlein J and Thrasher JB: Macrophage inhibitory cytokine-1: possible bridge molecule of inflammation and prostate cancer. Cancer Res 69: 2-5, 2009.
42. Svaren J, Ehrig T, Abdulkadir SA, Ehrengruber MU, Watson MA and Milbrandt J: EGR1 target genes in prostate carcinoma cells identified by microarray analysis. J Biol Chem 275: 38524-38531, 2000.
43. Shim M and Eling TE: Protein kinase C-dependent regulation of NAG-1/placental bone morphogenic protein/MIC-1 expression in LNCaP prostate carcinoma cells. J Biol Chem 280: 18636-18642, 2005.
44. Mora GR, Olivier KR, Mitchell RF, Jr., Jenkins RB and Tindall DJ: Regulation of expression of the early growth response gene-1 (EGR-1) in malignant and benign cells of the prostate. Prostate 63: 198-207, 2005.

Table I. Demographics and clinical parameters of prostate tissues, and number of images analyzed. A total of 14 adenocarcinomas (tumor), 16 tumor adjacent tissues (adjacent), and 9 disease-free tissues were analyzed. In total, 488 images were queried (numbers for each case and marker are indicated). Specimens were collected at the University of New Mexico Hospital (UNMH, Albuquerque NM) or obtained from the Cooperative Human Tissue Network (CHTN; Nashville TN).

Prostate tissues	**Age**	**TNM [1]**	**Gleason**	**Number of images analyzed [3]**			
Disease-free (CHTN)				**EGR-1**	**MIC-1**	**PDGF-A**	**FASN**
1	26			3	3	--	3
2	43			3	3	--	3
3	46			3	--	3	4
4	79			3	4	2	--
5	43	not applicable		3	3	3	4
6	55			3	3	2	4
7	55			3	--	--	4
8	45			3	--	--	3
9	n/a [2]			3	--	--	--
			Total =	**27**	**16**	**10**	**25**

Tumor and adjacent (UNMH/CHTN) [4]	**Age**	**TNM [1]**	**Gleason**	**Tumor**				**Adjacent**			
				EGR-1	**MIC-1**	**PDGF-A**	**FASN**	**EGR-1**	**MIC-1**	**PDGF-A**	**FASN**
1	51	n/a [2]	7 (3+4)	--	3	--	--	--	--	--	--
2	54	T3a	7 (3+4)	--	3	--	--	--	--	--	--
3 (m)	59	T3b	9 (4+5); 6 (3+3)	3	3	3	3	3	3	3	3
4 (m)	63	T3a	6 (4+3)	--	5	2	--	--	3	3	--
5 (m)	69	T2c	7 (4+3)	3	3	6	3	6	3	3	3
6 (m)	68	T3b	8 (5+3)	3	4	3	3	3	3	3	3
7 (m)	55	T2c	8 (3+5)	3	6	9	--	6	6	--	--
8 (m)	57	T3a	7 (4+3)	3	3	3	3	3	3	3	3
9 (m)	55	T2c	8 (3+5)	3	--	3	3	6	--	3	9
10 (m)	54	T2-T3	6 (3+3)	--	--	--	3	6	--	6	6
11	54	T2c	6 (3+3)	--	--	--	--	9	--	5	9
12 (m)	64	T3b	6 (3+3)	3	--	4	--	9	--	4	--
13	62	T2c	6 (3+3)	--	--	--	--	9	9	9	16
14 (m)	62	T3b	7 (4+3)	3	4	3	4	6	5	3	9
15 (m)	44	T2c	6 (3+3)	3	--	3	4	5	--	--	6
16	58	T2c	9 (4+5)	--	--	--	--	9	--	--	10
17	69	T2c	6 (3+3)	--	--	--	--	9	--	--	12
18 (m)	68	T3a	7 (3+4)	3	3	3	4	3	6	--	4
			Total =	**30**	**37**	**42**	**30**	**92**	**41**	**45**	**93**

[1] Tumor Nodes Metastasis (TNM) pathological stage was assigned using criteria published by the American Joint Committee on Cancer (https://cancerstaging.org/Pages/default.aspx).

[2] n/a, not available.

[3] "--" indicates no available images of sufficient quality.

[4] "(m)" indicates tumors that were matched with their corresponding adjacent tissues.

Figure 1A

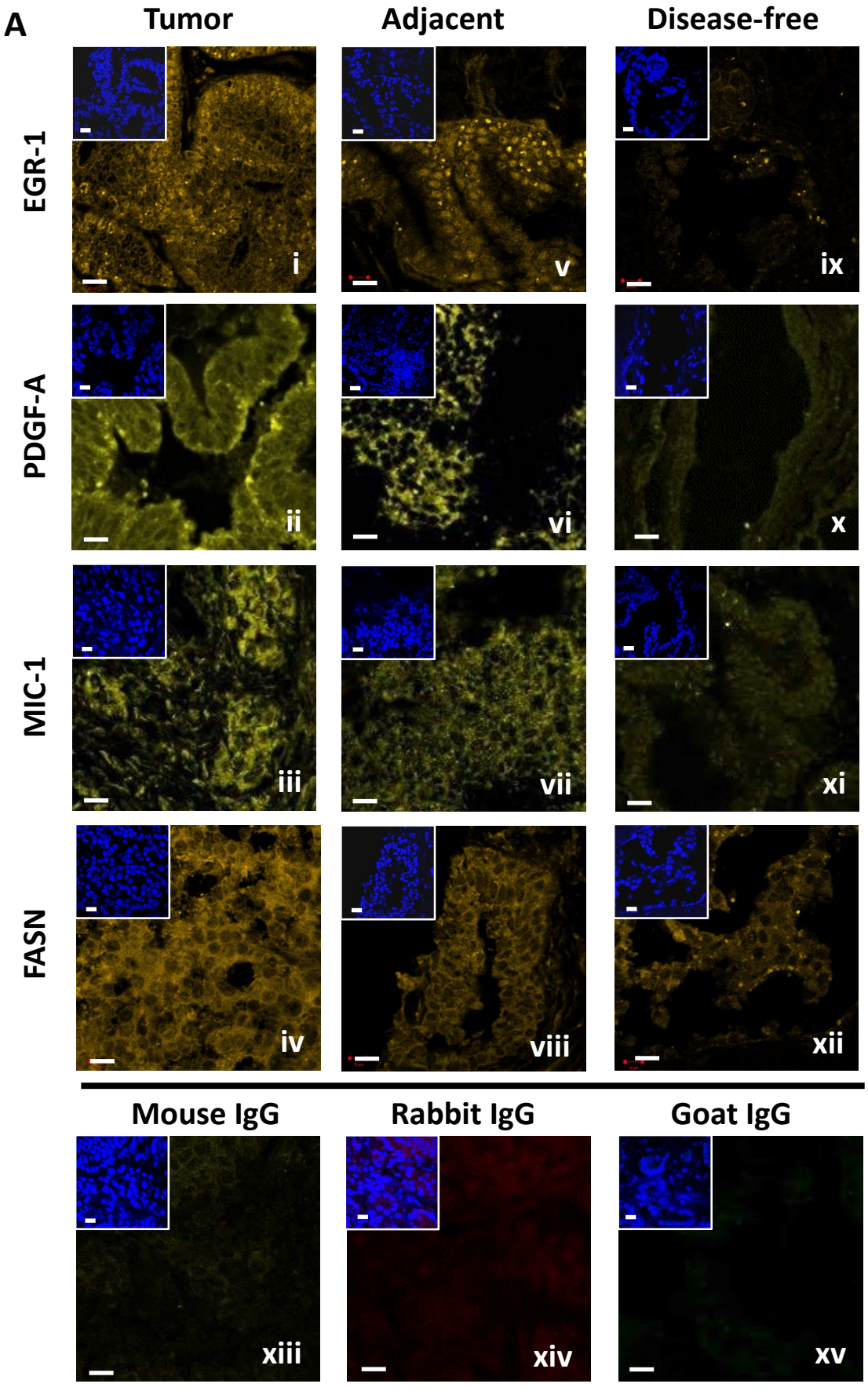
A
Tumor
Adjacent
Disease-free
EGR-1
PDGF-A
MIC-1
FASN
i
ii
iii
iv
v
vi
vii
viii
ix
x
xi
xii
Mouse IgG
Rabbit IgG
Goat IgG
xiii
xiv
xv

Figure 1B

B

Whole slide data acquisition

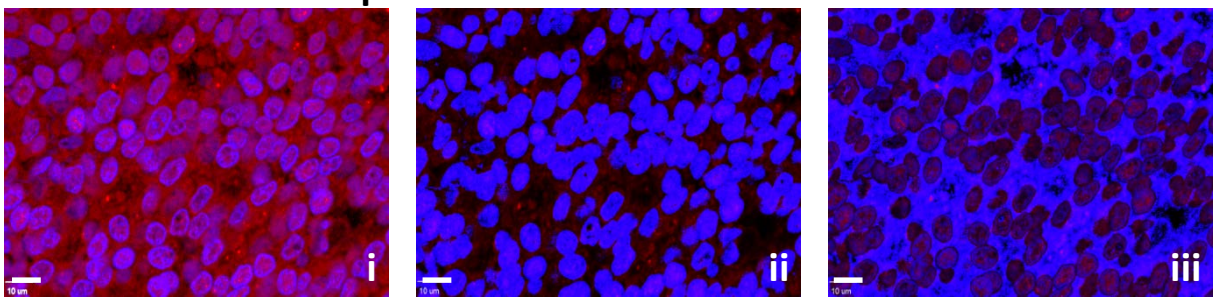

Region of interest data acquisition

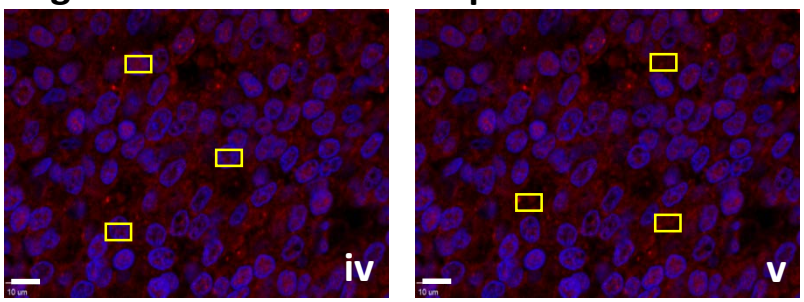

Figure 2

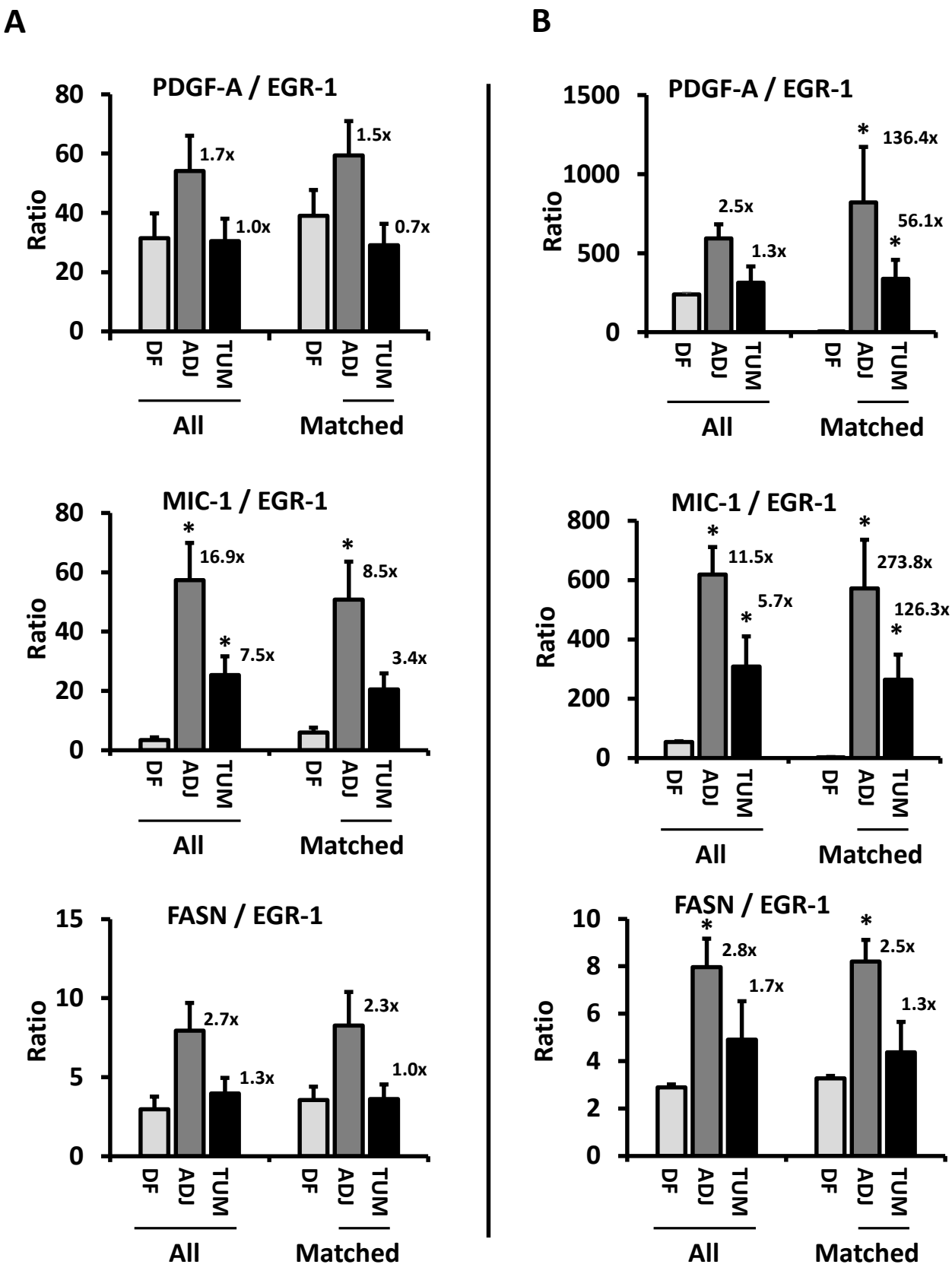
A
B
PDGF-A / EGR-1
Ratio
80
60
40
20
0
1.7x
1.0x
1.5x
0.7x
DF
ADJ
TUM
All
Matched
MIC-1 / EGR-1
16.9x
7.5x
8.5x
3.4x
FASN / EGR-1
15
10
5
2.7x
1.3x
2.3x
1.0x
1500
1000
500
2.5x
1.3x
136.4x
56.1x
800
600
400
200
11.5x
5.7x
273.8x
126.3x
2.8x
1.7x
2.5x
1.3x

Figure 3

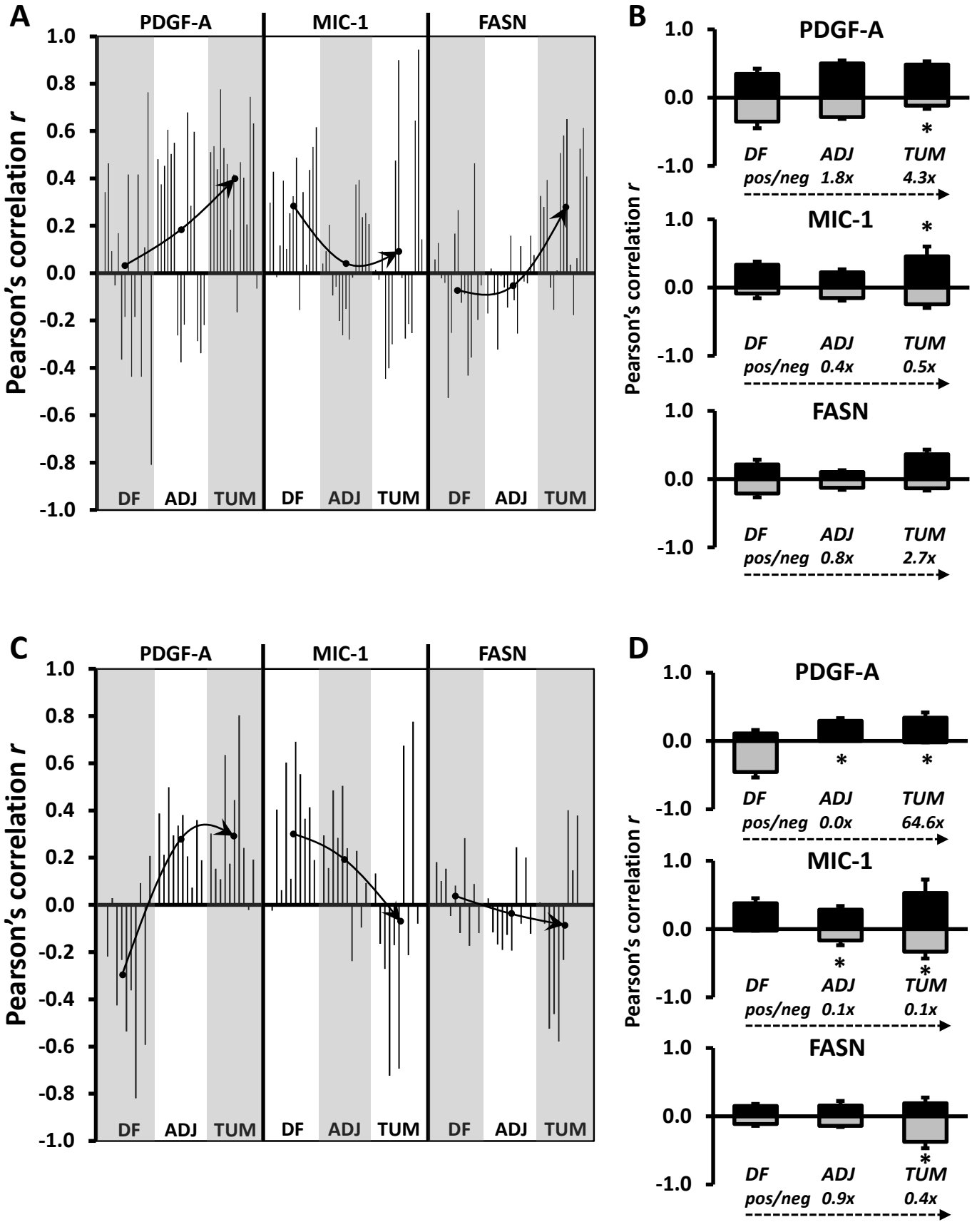
A
PDGF-A
MIC-1
FASN
Pearson's correlation r
1.0
0.8
0.6
0.4
0.2
0.0
-0.2
-0.4
-0.6
-0.8
-1.0
DF
ADJ
TUM
B
PDGF-A
DF ADJ TUM
pos/neg 1.8x 4.3x
MIC-1
DF ADJ TUM
pos/neg 0.4x 0.5x
FASN
DF ADJ TUM
pos/neg 0.8x 2.7x
C
PDGF-A
MIC-1
FASN
D
PDGF-A
DF ADJ TUM
pos/neg 0.0x 64.6x
MIC-1
DF ADJ TUM
pos/neg 0.1x 0.1x
FASN
DF ADJ TUM
pos/neg 0.9x 0.4x

Figure 4A

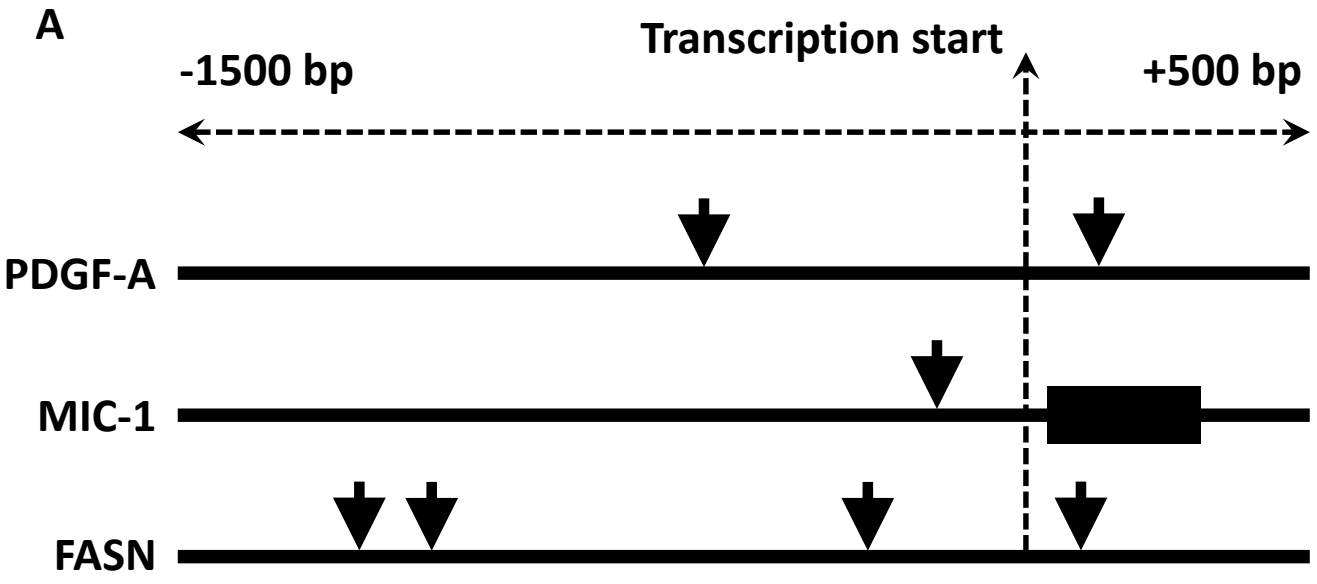

Figure 4B and 4C